Mechanical Resonance Dispersion in Metals at Audio-Frequencies

EDWIN R. FITZGERALD
Department of Physics, Pennsylvania State University, University Park, Pennsylvania
(Received May 24, 1957)

Measurements of the complex shear compliance ($\mathbf{J}^*=J'-iJ''$) of pure, polycrystalline lead, indium, and aluminum at closely spaced frequencies in the audio-frequency range have resulted in the discovery of multiple frequency dispersions of the resonance type. Values of the loss compliance (J'') are found to have sharply defined maxima in the range from 100 to 5000 cps; values of the storage compliance (J') rise to a maximum and then drop to pass through a minimum as a narrow (50 to 100 cps wide) dispersion region is traversed in the direction of increasing frequency. The shapes of the complex compliance *vs* frequency curves are thus similar to those found for the variation of the complex index of refraction with frequency (in absorption bands) at infrared and optical frequencies. The results indicate the presence of a dispersion mechanism different from those leading to the relaxation dispersions previously observed in connection with the mechanical properties of metals. Results on lead indicate that some of the resonances can be eliminated by high-temperature annealing of the sample material. The possibility that dislocation vibrations are responsible for the observed phenomena is considered, but no specific mechanism is found to explain the results. A number of dislocation theories are examined but these fail to predict any mechanical resonance dispersion at audio-frequencies. In addition to their theoretical implications, the results are believed to be of considerable practical importance since they indicate that certain materials when subject to mechanical vibrations of relatively low frequencies may undergo large changes in modulus at a particular frequency or frequencies.

I. INTRODUCTION

IF a material such as a polycrystalline metal or crystalline polymer is subjected to a dynamic shearing stress of the form $s=s_0\sin(2\pi ft)$, a periodic strain of the same frequency, f, results. In general this strain is out of phase with the stress as described by $a=a_0\sin(2\pi ft-\delta)$ where δ is the phase difference between the applied stress and the resulting strain. The ratio between the strain amplitude, a_0, and the stress amplitude, s_0, is called the absolute dynamic compliance J. Thus J and δ are quantities which describe the dynamic mechanical behavior of a material in shear. Two alternate quantities, J', and J'' can be used in place of J and δ by considering the strain to be divided into two parts, one of which is in phase with the applied stress, and the other of which is 90° out of phase.

$$a=s_0[J'\sin\omega t-J''\cos\omega t],$$

where

$$J=[(J')^2+(J'')^2]^{\frac{1}{2}} \quad \text{and} \quad J''/J'=\tan\delta.$$

This is equivalent to considering the compliance to be a complex quantity $\mathbf{J}^*=J'-iJ''$ where the storage compliance, J', is a measure of the elastic energy stored and recovered during each cycle of deformation and the loss compliance, J'', is proportional to the energy dissipated during each cycle.

In considering the variation of compliance with frequency it is convenient to distinguish between two types of dispersion; (1) relaxation or retardation dispersion, and (2) resonance dispersion. In the first case the frequency dependence of the compliance is similar to that of the mechanical model of Fig. 1(a) in which an ideal spring of modulus G_0, and a dashpot of viscosity η_0 are in series with a retarded spring of modulus G and viscosity η. The spring of modulus G_0 represents an instantaneous elastic response, while the spring of modulus G is retarded by the dashpot of viscosity η; the ratio η/G is called the retardation time τ. The dashpot of viscosity η_0 corresponds to permanent deformation which may result from plastic flow. The storage compliance and loss compliance of this mechanical model, when subjected to a sinusoidal stress of frequency $\omega/2\pi$, are

$$J'=\frac{1}{G_0}+\frac{1}{G}\left(\frac{1}{1+\omega^2\tau^2}\right),$$
$$J''=\frac{1}{\omega\eta_0}+\frac{1}{G}\left(\frac{\omega\tau}{1+\omega^2\tau^2}\right). \tag{1}$$

The dependence of J' and J'' on ω as calculated from Eq. (1) is shown in Fig. 1(b). This type of frequency variation of mechanical properties has been found for polycrystalline metals and alloys by various investigators[1–5] but in most cases the variation of mechanical properties has been studied as a function of temperature

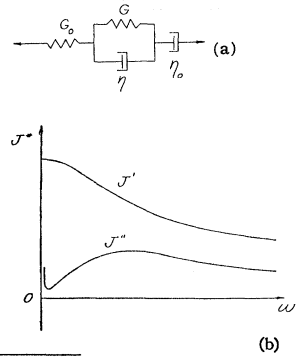

FIG. 1. (a) Mechanical model for relaxation dispersion. (b) Frequency dependence of shear compliance for relaxation dispersion.

[1] R. Kamel, Phys. Rev. **75**, 1606 (1949).
[2] K. Bennewitz and H. Rötger, Z. tech. Physik **19**, 521 (1938).
[3] W. P. Mason and H. J. McSkimin, J. Appl. Phys. **19**, 940 (1948).
[4] A. L. Kimball and D. E. Lovell, Phys. Rev. **30**, 948 (1927).
[5] J. A. Sauer, Virginia J. Sci. **5**, 144 (1954).

at a constant (or slightly varying) frequency.[6–10] There are very few data reported giving the complex compliance (or modulus) as a function of closely spaced frequencies in the audio-frequency range. Various mechanisms[3,7,11,12] have been advanced to account for relaxation (or retardation) dispersion in metals including (a) thermoelastic damping, (b) stress-induced diffusion, (c) grain-boundary slip, (d) plastic flow and (e) lattice-wave scattering. A much broader relaxation dispersion has been observed in the case of plastic materials such as linear amorphous polymers[13–16] where the model of Fig. 1(a) must be replaced by a series of retarded spring elements having a distribution of retardation times in order to represent the experimental data.[17–19]

In the case of resonance dispersion the frequency dependence of the complex compliance is similar to that of the mechanical model of Fig. 2(a). The quantity m/l represents the *effective* mass per unit length of the retarded spring and all other elements have the same significance as in the previous model of Fig. 1(a). In this case the dependence of the storage compliance and the loss compliance on the frequency, $\omega/2\pi$, of an applied sinusoidal stress are

$$J'=\frac{1}{G_0}+\frac{1}{G}\left(\frac{(1-\omega^2/\omega_r^2)}{(1-\omega^2/\omega_r^2)^2+\omega^2\tau^2}\right),$$
$$J''=\frac{1}{\omega\eta_0}+\frac{1}{G}\left(\frac{\omega\tau}{(1-\omega^2/\omega_r^2)^2+\omega^2\tau^2}\right), \tag{2}$$

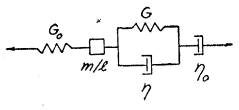

(a)

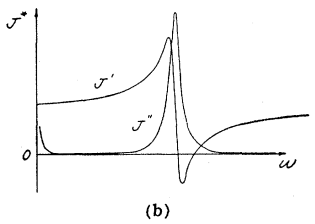

(b)

FIG. 2(a). Mechanical model for resonance dispersion. (b) Frequency dependence of shear compliance for resonance dispersion.

where $\omega_r=[G/(m/l)]^{\frac{1}{2}}$ is the resonant frequency. The dependence of J' and J'' on ω as predicted from Eq. (2) is shown in Fig. 2(b). In this case a maximum followed by a minimum occurs in the J' *vs* ω curve while J'' rises to a maximum in the vicinity of $\omega=\omega_r$. There are no previous data published showing this type of frequency variation of compliance at audio-frequencies for either metals or polymers although a dislocation theory of Granato and Lücke[20] predicts resonances in metals at frequencies of the order of 50 to 500 Mc/sec.

In this investigation the variations of J' and J'' with frequency for pure polycrystalline metals are determined for sinusoidal shearing stresses at frequencies from 100 to 5000 cps and at strains sufficiently small so that the results are amplitude independent. Experimental results for aluminum, lead, and indium demonstrate the existence of multiple dispersion regions of the resonance type.

II. DETERMINATION OF COMPLEX SHEAR COMPLIANCE

Measurements of complex shear compliance were made by the electromagnetic transducer method of Fitzgerald and Ferry.[13] While this method has been extensively used for determining dynamic mechanical properties of plastic and rubber-like materials, the present work is the first instance of its use for metals. A brief description of the method is presented with particular emphasis on its adaptation to metals and with some details of the construction of an improved version of the original apparatus.

1. General Method

The transducer method used measures mechanical impedance in terms of electrical resistance and capacitance. A rigid metal tube with coils wound around the ends is suspended by eight long phosphor bronze wires (0.010-in. diam) so that it is free to move axially but so that the coils are firmly centered in annular gaps in which radial magnetic fields are produced by a permanent magnet. Alternating currents are passed through the coils and the consequent vibration is modified by pressing two disks of the material to be tested against the tube from a supended inner core of large mass. From determinations of the mechanical impedance of the system with and without the samples the impedance of the samples alone is found. The equivalent mechanical circuit diagram of the apparatus is shown in Fig. 3. In order to determine that part of the total impedance (or admittance) due to the samples alone two subtractions must be made: the mechanical impedance due to the driving tube, $\mathbf{Z}_{Mt}$ (including its mass, the effects of the support wires, air resistance, etc.), is subtracted from the total measured impedance $\mathbf{Z}_M$ to give an impedance $\mathbf{Z}_{AB}$; then from the admittance $\mathbf{Y}_{AB}$ $(=1/\mathbf{Z}_{AB})$ there must be subtracted a small background

[6] Y. L. Yousef and R. Kamel, J. Appl. Phys. **25**, 1064 (1954).
[7] T. S. Kê, Phys. Rev. **71**, 533 (1947); **72**, 41 (1947).
[8] T. S. Kê, J. Appl. Phys. **21**, 414 (1950).
[9] C. A. Wert, J. Appl. Phys. **26**, 640 (1955).
[10] W. Koster and K. Rosenthal, Z. Metallkunde **30**, 345 (1938).
[11] C. Zener, Phys. Rev. **52**, 230 (1937); *Elasticity and Anelasticity of Metals* (University of Chicago Press, Chicago, 1948).
[12] H. Kolsky, *Stress Waves in Solids* (Clarendon Press, Oxford, 1953).
[13] E. R. Fitzgerald and J. D. Ferry, J. Colloid Sci. **8**, 1 (1953).
[14] Fitzgerald, Grandine, and Ferry, J. Appl. Phys. **24**, 650 (1953).
[15] M. L. Williams and J. D. Ferry, J. Colloid Sci. **9**, 479 (1954).
[16] L. D. Grandine and J. D. Ferry, J. Appl. Phys. **24**, 679(1953).
[17] T. Alfrey and P. Doty, J. Appl. Phys. **16**, 700 (1945).
[18] J. D. Ferry, J. Am. Chem. Soc. **72**, 3746 (1950).
[19] Ferry, Grandine, and Fitzgerald, J. Appl. Phys. **24**, 911 (1953).
[20] A. Granato and K. Lücke, J. Appl. Phys. **27**, 583 (1956).

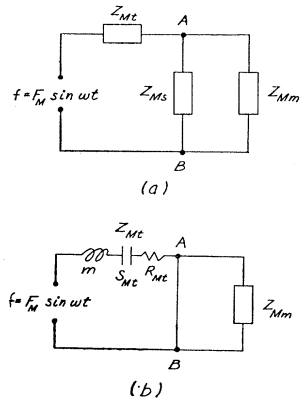

FIG. 3. (a) Mechanical circuit diagram for transducer with samples. $\mathbf{Z}_{Mt}$ is the mechanical impedance of the suspended driving tube, $\mathbf{Z}_{Ms}$ is the mechanical impedance of the sample disks, and $\mathbf{Z}_{Mm}$ that of the large suspended mass against which the samples are sheared. (b) Mechanical circuit diagram for transducer without samples, driving tube not clamped to mass.

admittance $\mathbf{Y}_{Mm}$ resulting from the effective admittance of the large suspended mass against which the sample is sheared. The mechanical admittance of the samples is given by

$$\mathbf{Y}_{Ms}=\mathbf{Y}_{AB}-\mathbf{Y}_{Mm} \quad \text{where} \quad \mathbf{Y}_{AB}=1/(\mathbf{Z}_M-\mathbf{Z}_{Mt}),$$

and the complex compliance $\mathbf{J}^*$ is then found from the relation

$$\mathbf{J}^*=-i\mathbf{Y}_{Ms}C/\omega, \tag{3}$$

where C is a coefficient depending on the shape and dimension of the sample disks, and ω is the circular frequency. In order to obtain maximum precision, an optimum sample size is chosen so that

$$\mathbf{Z}_{Mt}\ll\mathbf{Z}_{Ms} \quad \text{and} \quad \mathbf{Y}_{AB}\gg\mathbf{Y}_{Mm};$$

for precise results over a wide frequency and temperature range several sample sizes may be necessary.

2. Electrical Measuring Circuit

The mechanical impedance, $\mathbf{Z}_M$, of the transducer is measured by means of the electrical circuit shown in Fig. 4. One of the driving-tube coils ($2A$) is placed in the arm of a bridge where it acts as a dynamic impedance $\mathbf{Z}_2$, while the other driving coil ($1A$) in series with a resistance, R_A, parallels the bridge circuit. For a particular setting of C_4 and R_3 the bridge is balanced by adjusting R_1 and C_1; at balance $\mathbf{Z}_2=\mathbf{Z}_3\mathbf{Z}_1/\mathbf{Z}_4$. The impedance $\mathbf{Z}_2$ equals the (vector) sum of the intrinsic impedance $\mathbf{Z}_2^0$ of coil $2A$ and an effective impedance $\mathbf{E}_2/\mathbf{I}_2$, where $\mathbf{E}_2$ is the back emf generated as a result of the motion of coil $2A$ in the magnetic field. Thus

$$\mathbf{Z}_2=\mathbf{Z}_2^0-B_2l_2\mathbf{V}/\mathbf{I}_2, \tag{4}$$

where l_2 is the length of wire of coil $2A$ in the radial magnetic field of flux density B_2, $\mathbf{V}$ is the velocity of the driving tube, and $\mathbf{I}_2$ is the current in coil $2A$. Now $\mathbf{V}=\mathbf{F}/\mathbf{Z}_M$, where $\mathbf{F}$ is the total applied force and $\mathbf{Z}_M$ is the total mechanical impedance presented by the moving system. $\mathbf{F}$ is the (vector) sum of the forces on coil $1A$ and coil $2A$ given by $\mathbf{F}=B_1l_1\mathbf{I}_1+B_2l_2\mathbf{I}_2$; or if we let $B_1l_1=K_1$, $B_2l_2=K_2$ and $K_1/K_2=a$, the force is $\mathbf{F}=K_2(a\mathbf{I}_1+\mathbf{I}_2)$ so that the electrical impedance [Eq. (4)] becomes

$$\mathbf{Z}_2=\mathbf{Z}_2^0-[K_2^2(a\mathbf{I}_1/\mathbf{I}_2+1)/\mathbf{Z}_M], \tag{5}$$

and, if we replace the complex ratio $\mathbf{I}_1/\mathbf{I}_2$ by $\mathbf{r}$, the final form of the expression becomes

$$\mathbf{Z}_2=\mathbf{Z}_2^0-[K_2^2(1+a\mathbf{r})/\mathbf{Z}_M]. \tag{6}$$

In order to eliminate the necessity of determining $\mathbf{Z}_2^0$ from "clamped" measurements, the electrical impedance $\mathbf{Z}_2$ is found for two values of the ratio $\mathbf{r}$ and the mechanical impedance or admittance is found from the difference between the electrical impedances:

$$\mathbf{Z}_{12}\equiv[(\mathbf{Z}_2)_1-(\mathbf{Z}_2)_2]/(\mathbf{r}_2-\mathbf{r}_1)=K^2/\mathbf{Z}_M,$$

or

$$\mathbf{Y}_M=1/\mathbf{Z}_M=\mathbf{Z}_{12}/K^2, \tag{7}$$

where $aK_2^2=K^2$. In practice R_3 and R_A are made very large compared to the dynamic impedances of coils $2A$ and $1A$ so that the approximation $\mathbf{r}\cong R_3/R_A$ is valid.

The current ratio can be varied by changing either R_3 or R_A or both, but keeping them large compared to the dynamic electrical impedances of coils $2A$ and $1A$. For the case where the current ratio is changed by varying R_A only, the determination is independent of the value of R_3. For maximum precision the differences in dynamic electrical impedances should be large and this can be accomplished by making the differences in r large.

The emf in coil $2A$ resulting from the mutual inductance of coils $1A$ and $2A$ is eliminated by a shielding coil $1B$ wound on the inside of a coil form placed around coil $1A$ but not touching it. The shielding coil is fixed to the pole piece of the magnet and placed in electrical parallel with coil $1A$; the shielding coil current is adjusted by means of the components R_B, C_B, and L_B until the induced emf in coil $2A$ due to coil $1A$ is exactly canceled by the induced emf of coil $1B$. In order to determine the null condition a fourth stationary test coil, $2B$, is placed inside a coil form just surrounding coil $2A$ and placed across the detector while the bridge circuit is open. Because of the nearly identical locations of coils $2B$ and $2A$ it is assumed that when the induced emf in $2B$ is zero the emf in coil $2A$ is zero also. This adjustment is made at each frequency before determining $\mathbf{Z}_2$ and assures that only motional emf is present

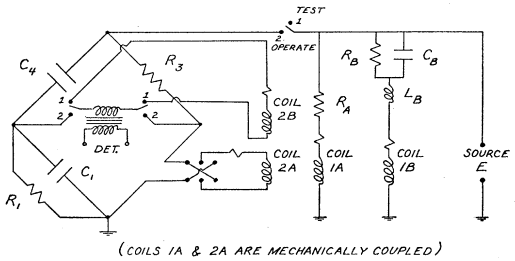

FIG. 4. Electrical circuit for measuring mechanical impedance.

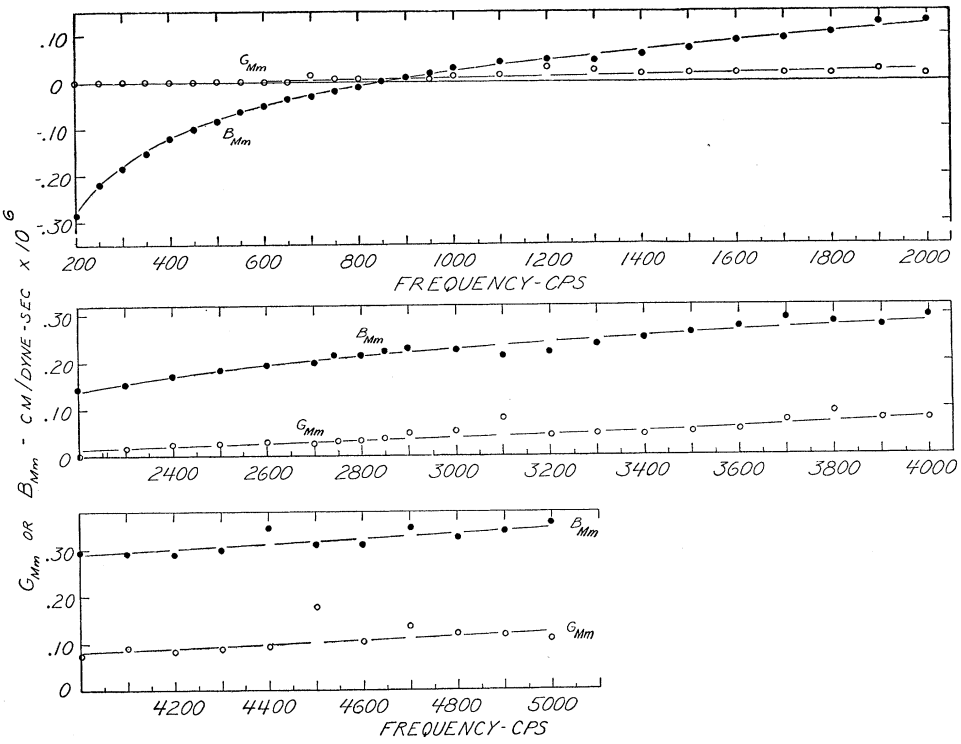

FIG. 5. Frequency dependence of mechanical admittance of transducer I with driving tube and suspended mass clamped directly together (no sample).

in coil $2A$ as was tacitly assumed in the previous discussion.

3. Calibration of the Apparatus

The transducer constant K^2 is determined from measurements of the mechanical impedance of the driving-tube system without samples [Fig. 3(b)]. In this case the electrical admittance $(1/\mathbf{Z}_{12})$ is

$$\mathbf{Y}_{12}{}^0=G_{12}{}^0+iB_{12}{}^0=\mathbf{Z}_{Mt}/K^2.$$

The mechanical impedance, in turn, is $\mathbf{Z}_{Mt}=R_{Mt}+i(\omega m-S_{Mt}/\omega)$ where R_{Mt} is a small residual mechanical resistance due to stretching of the support wires, air resistance, or other effects; m is the mass of the coils and tube; S_{Mt} is a small elastance associated with the eight support wires. Then

$$G_{12}{}^0=R_{Mt}/K^2;\quad B_{12}{}^0=(\omega m-S_{Mt}/\omega)/K^2,$$

and a plot of $\omega B_{12}{}^0$ *vs* ω^2 should give a straight line of slope m/K^2 and intercept S_{Mt}/K^2. Experimental data taken at 60 frequencies from 25 to 5000 cps on transducer I yield a value of $K^2=2.13\times10^5$ ohms dyne-sec/cm, constant to within $\pm4\%$; data taken at 30 frequencies from 25 to 8000 cps on transducer II give a value of $K^2=1.75\times10^5$ ohms dyne-sec/cm, constant to within $\pm2\%$.[21]

The mechanical admittance $\mathbf{Y}_{Mm}$ associated with the large suspended mass is determined from measurements made with the sample holders of this part of the apparatus clamped against the flat portions of the driving tube. Under such conditions the driving tube and suspended mass should move as a single rigid unit [in Fig. 3(a) equivalent to $\mathbf{Z}_{Ms}=\infty$] with the mechanical admittance of the clamped system essentially going to zero as the frequency is increased. This clamped condition or "floating mass" calibration is the most severe test to which the apparatus can be subjected; any nonrigidity of the sample holders, driving-tube resonances, slipping, stray resonances, or other spurious effects are most likely to appear under these conditions. The results of these tests are shown in Figs. 5 and 6 for transducers I and II where the measured mechanical admittance $\mathbf{Y}_{Mm}=G_{Mm}-iB_{Mm}$ is plotted *vs* frequency. The ordinate scale is the same as that used later is giving the experimental results obtained with samples of polycrystalline metals; it is apparent that no irregular effects of appreciable magnitude are observed. Values of B_{Mm} rise from large negative values to values close to zero as the frequency increases. If the floating mass-driving tube unit is an ideally rigid mass, then $B_{Mm}\cong-1/\omega M$ and should rise from a large negative value to approach zero as the frequency increases. Actually values of B_{Mm} become slightly positive above about 1200 cps, indicating a small residual compliance in the driving tube–floating mass clamped system. For transducer I values of B_{Mm} reach 0.35×10^{-6} cm/dyne-sec at 5000 cps, while for transducer II values of B_{Mm} rise to 0.22×10^{-6} cm/dyne-sec at 5000 cps. These values are, however, less than 10% (less than 5% for transducer II) of the values of B_{Ms} obtained with the metal

[21] The instrument has two separate shearing units, designated transducers I and II, in a common housing as is explained in Sec. 4 and shown in Fig. 7.

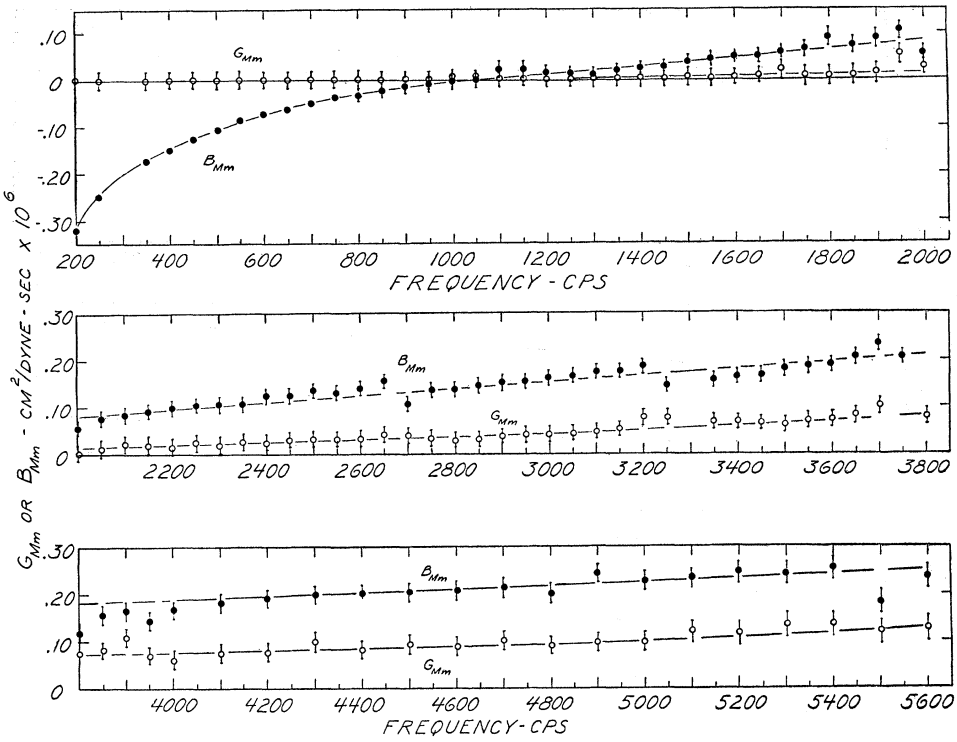

FIG. 6. Frequency dependence of mechanical admittance of transducer II with driving tube and floating mass clamped directly together (no sample).

samples so that the floating-mass calibration is not critical. From the standpoint of the data to be presented here, the most important feature of these clamped measurements is the complete absence of any resonances or large deviations from the predicted behavior of the system is either transducer.

4. Description of Transducer

The electromagnetic transducer used in these measurements is shown in a cross-section drawing in Fig. 7. Two sample disks are pressed outward by stainless steel slabs against the inside flat sections of the driving tube; enough pressure is applied to prevent slipping and then the jaws of the sample slabs (holders) are clamped against V ways in the floating-mass housing by means of two $\frac{3}{8}$-in. diam machine screws. The dynamic shear measurements are thus carried out while the sample is under a constant static compressive strain (and hence some stress) at right angles to the direction of shear. The distance between the driving-tube flats and the sample slabs is measured by using two stainless steel micrometer heads reading to 0.0001 in. to give the sample thicknesses.

As can be seen from Fig. 7, the transducer has two separate shearing units to which the electrical measuring system can be alternately switched. This is convenient in measurements carried out as a function of time or temperature, as it allows two different samples to reach equilibrium conditions simultaneously. At the present time, transducer I has a driving tube made from 61ST6 aluminum, while transducer II has a driving tube of 75ST aluminum (a higher modulus alloy) and has thicker walls, additional reinforcing ribs, and a shorter nonconducting extension for coil $2A$. The calibration data previously cited indicate that driving tube II is more rigid than driving tube I, giving a more ideal behavior, particularly at high frequencies.

5. Temperature Control and Measurement

The entire transducer is enclosed in a fluid-tight stainless steel housing so that it can be lowered into a constant temperature bath for measurements from -50 to $+150$°C. The bath temperature is controlled to within ± 0.2°C by means of a thermoswitch, but because of the large mass of the instrument the temperature variation within the instrument is generally less than ± 0.05°C.

The temperature of the driving tube measured by a two-junction constantan-copper thermocouple is taken as the sample temperature after enough time for thermal equilibrium has elapsed. The thermocouple junctions are located in the flat section of the driving tube less than 0.025 in. from the sample faces. In the present measurements, which were taken with the transducer out of the bath, variations in temperature during any series of measurements were less than ± 0.20°C.

III. EXPERIMENTAL RESULTS

Samples of pure polycrystalline metals were used to obtain the data reported in this section. The samples of lead and aluminum were machined to size from cast

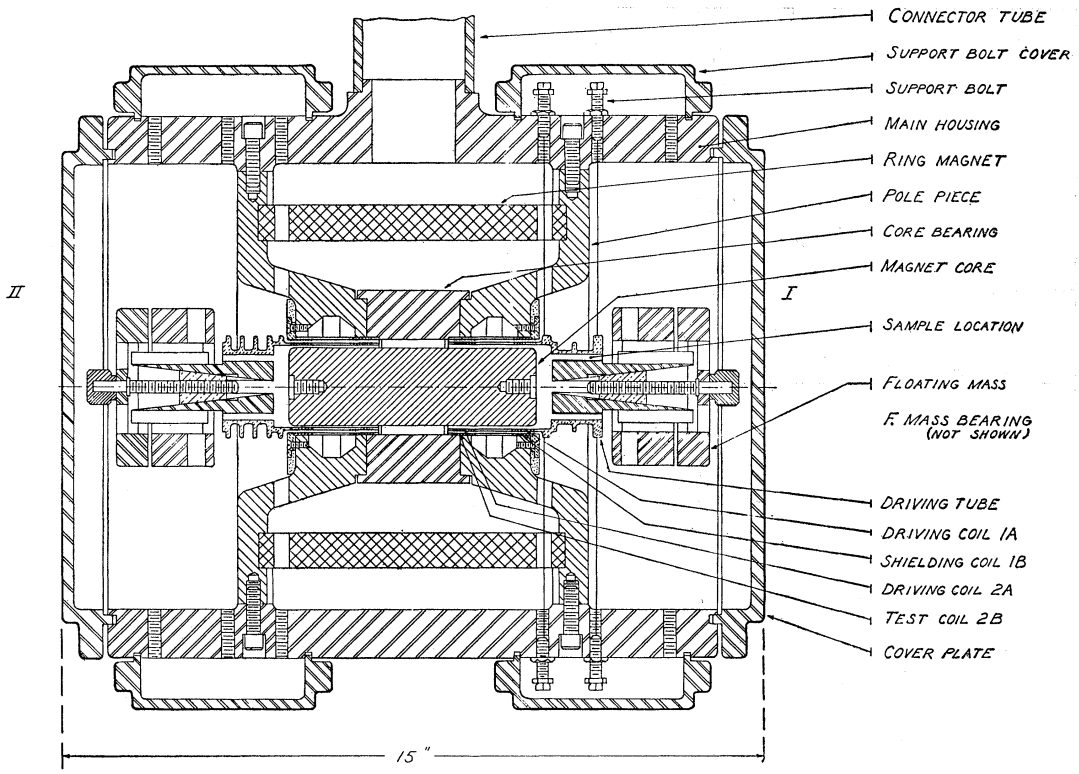

FIG. 7. Cross-section drawing (side view) of transducter.

bars, while the indium samples were formed by pouring the molten metal into a stainless-steel mold. A summary of the sample dimensions and analyses is given in Table I.

1. Lead

Samples of polycrystalline lead of 99.9995% purity (No. 22 see Table I) were compressed less than $\frac{1}{2}$% in the apparatus (transducer II) and measurements started at 100 cps 16.5 hours later. These were continued up to 2500 cps at 31.0 hours after the initial static compression. The frequency variation of complex shear compliance at 23.6°C is adduced in Fig. 8 for 200 to 2000 cps. Three dispersion regions are observed in this frequency range with resonant frequencies of 975, 1630, and 1870 cps. Values of J'' below 200 cps are too small to be measured accurately ($<0.005\times10^{-9}$ cm²/dyne); values of J' from 200 to 100 cps remain constant at approximately 0.19×10^{-9} cm²/dyne. J'' rises to a maximum value of 0.74×10^{-9} cm²/dyne near the resonant frequency of 975 cps; other features of

TABLE I. Sample dimensions and compositions.

Material	Lead				Indium	Aluminum
Purity %	99.9995				99.984	99.998
Analysis	Bi <0.0001% Cu 0.0001% Fe 0.0002%				Cu 0.006% Zn 0.01% Sn 0.01% Pb trace	Fe, Si, Cu <0.002%
Sample No.	22	22a[a]	25	27	23	24
Dimensions: diam. (in.)	0.250	0.250	0.376	0.250	0.384	0.250
thickness (in.)	0.199_5	0.199_2	0.150_8	0.201_2	0.208_0	0.198_9
Percent comp. in apparatus	<0.50	<0.50	<0.50	2.1	4.0	1.9
Sample coeff. C (cm) at 24°C[b]	1.25	1.25	3.74	1.25	3.00	1.30
Weight (grams)	1.810_8	1.810_8	3.101	1.827	2.815	0.429_2

[a] Sample 22 annealed in an air oven for 15 hours at 140–150°C.
[b] $C=A_1/h_1+A_2/h_2=2A/h$, where A_1 and A_2 are the cross-sectional areas and h_1 and h_2 the thicknesses of the sample disks.

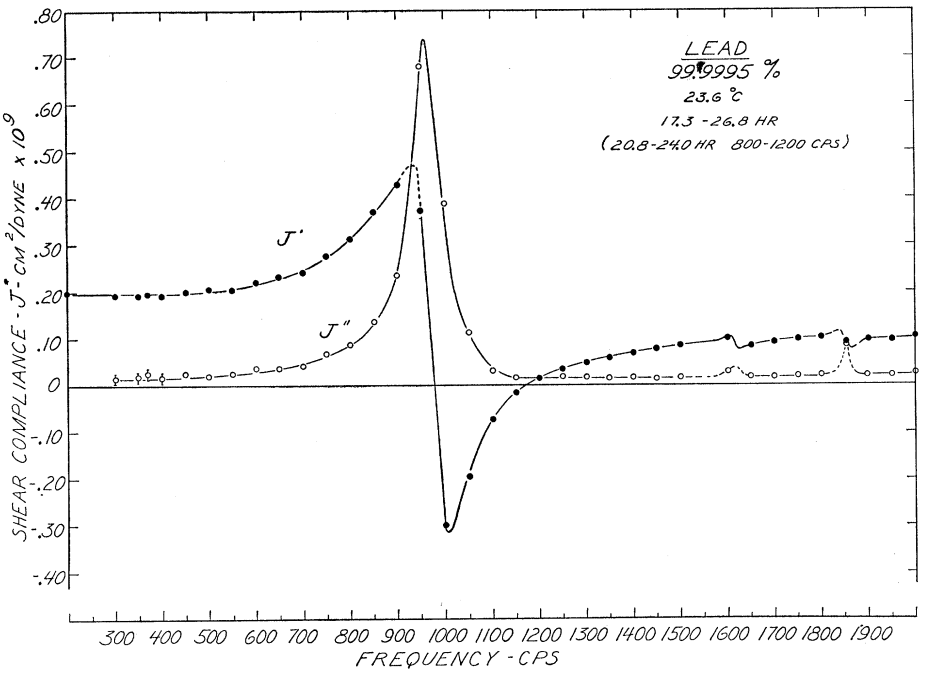

FIG. 8. Variation of the complex shear compliance ($J^*=J'-iJ''$) with frequency for polycrystalline lead at the time (~22 hr) and temperature indicated. Solid circles, J'; open circles, J''. Analysis of lead sample: Cu, 0.0001%; Fe, 0.0002%; Bi, <0.0001%; no other elements detected by chemical or spectrographic methods.

the dispersion are similar to the resonance type of dispersion shown in Fig. 2.

Another series of measurements started at 100 cps 116.0 hours after initial compression continued to 2100 cps at 129.2 hours; then was resumed at 2100 cps at 140.8 hours and continued to 4000 cps at 146.0 hours. Subsequently, measurements were taken from 4000 cps at 330.5 hours to 5000 cps at 356.5 hours. The variations of complex shear compliance with frequency at 23.5°C observed during this series of observations are shown in Figs. 9 and 10. The resonance originally found at 975 cps at approximately 22 hours shifts to 1030 cps at 118 hours with a decrease in the maximum value of J'' to 0.58×10^{-9} cm²/dyne (Fig. 9). Small resonances are again evident at 1630 cps and 1880 cps. Resonances are also observed (Fig. 10) at 2640 and 2890 cps; no dispersion is found from 3100 to 5000 cps.

A third set of measurements started at 100 cps 642.2

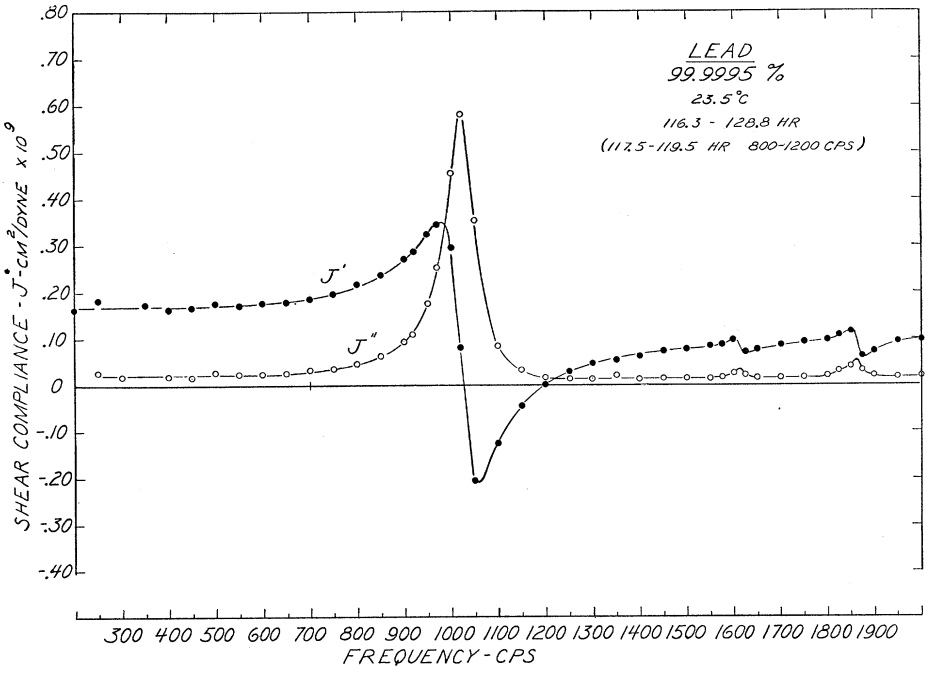

FIG. 9. Variation of the complex shear compliance ($J^*=J'-iJ''$) with frequency for the polycrystalline lead of Fig. 8 at the time (~118 hr) and temperature indicated. Solid circles, J'; open circles, J''.

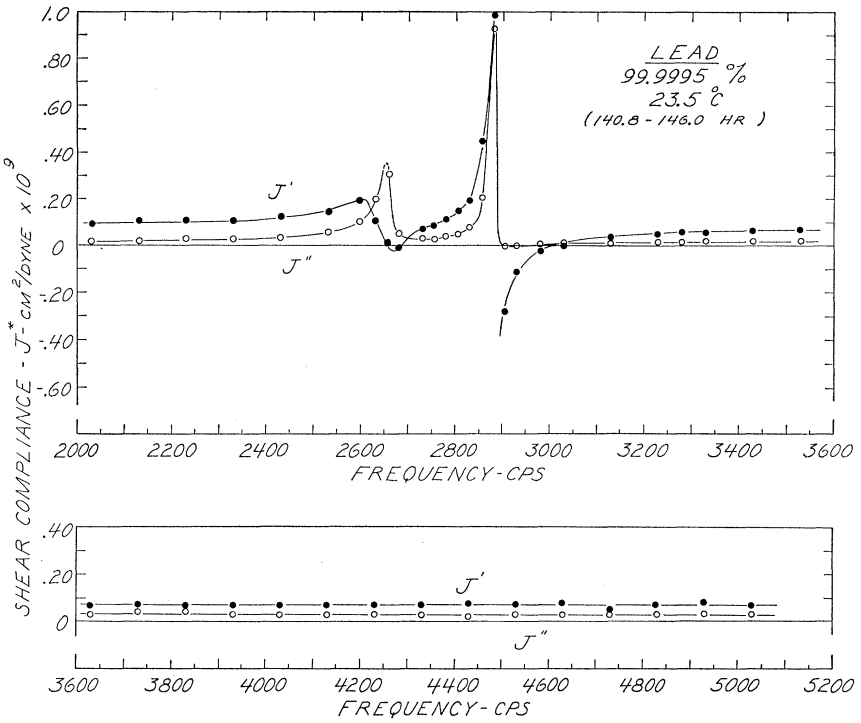

FIG. 10. Variation of the complex shear compliance ($J^*=J'-iJ''$) with frequency for the polycrystalline lead of Fig. 8 at the time and temperature indicated. Solid circles, J'; open circles, J''.

hours after compression continued to 2000 cps at 671.0 hours; this series was resumed at 2000 cps at 691.5 hours and concluded at 4000 cps at 722.8 hours. The results are given in Figs. 11 and 12. The resonance originally observed at 975 cps (at 22 hours) has shifted to 1150 cps with a decrease in maximum value of the loss compliance, J'', to 0.29×10^{-9} cm²/dyne. Small resonances are again found at 1630 cps and 1890 cps. The resonances at 2640 and 2890 cps are still present.

A fourth set of measurements from 200 to 2000 cps at 1339.0 to 1369.2 hours after insertion in the apparatus gave the results shown in Fig. 13. Resonances are evident at 1185, 1630, and 1890 cps. The maximum value of J'' at 1185 is 0.30×10^{-9} dyne/cm² or essentially the

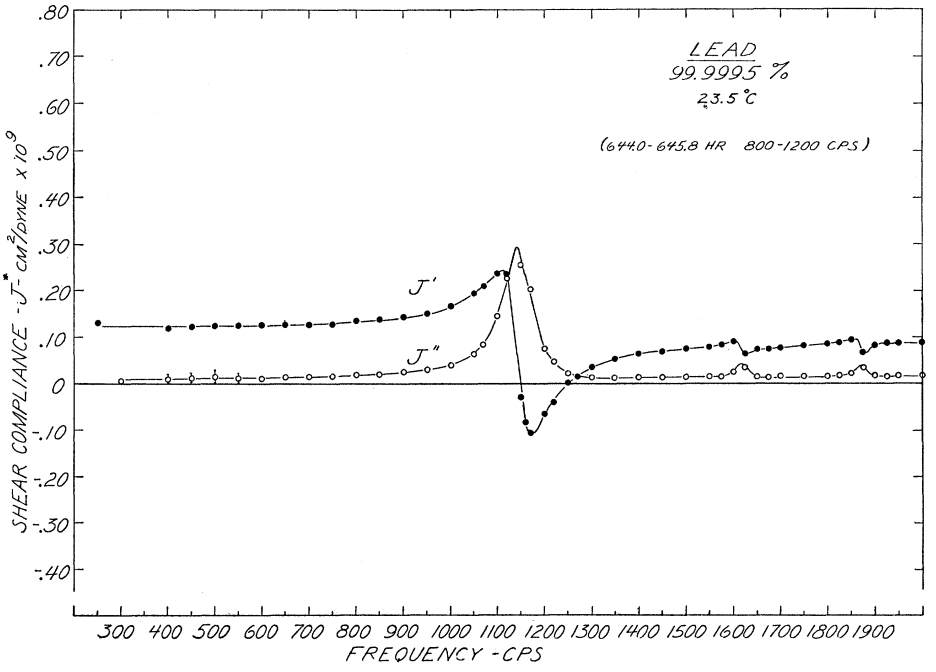

FIG. 11. Variation of the complex shear compliance ($J^*=J'-iJ''$) with frequency for the polycrystalline lead of Fig. 8 at the time (~644 hr) and temperature indicated. Solid circles, J'; open circles, J''.

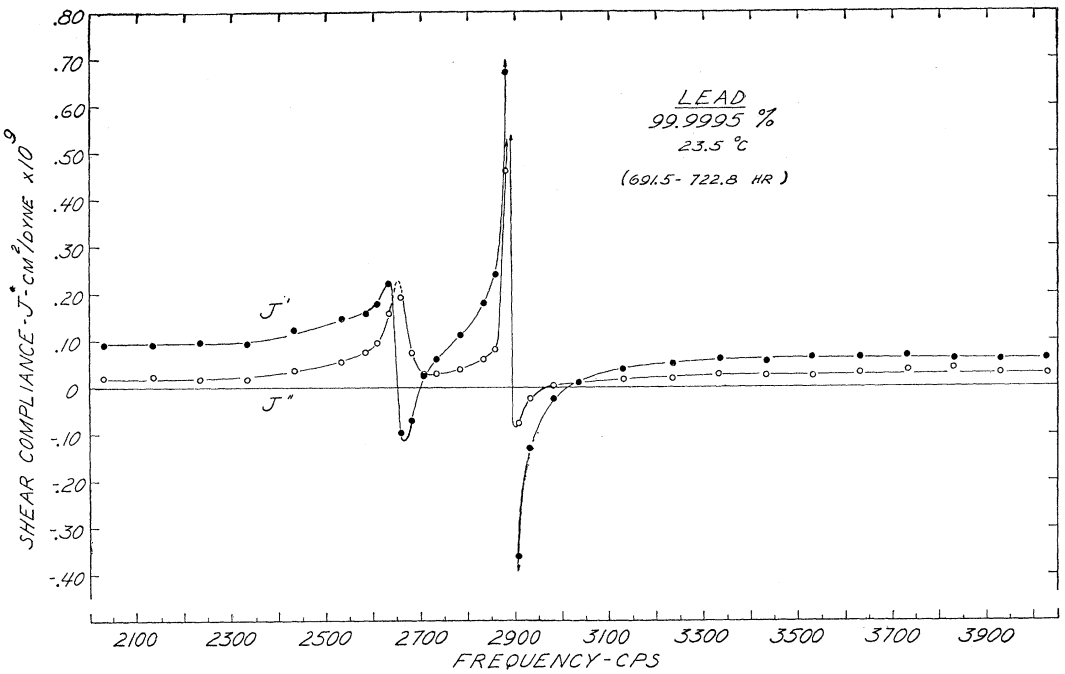

FIG. 12. Variation of the complex shear compliance ($\mathbf{J}^* = J' - iJ''$) with frequency for the polycrystalline lead of Fig. 8 at the time and temperature indciated. Solid circles, J'; open cirlces, J''.

same as that observed 600 hours earlier, although the resonant frequency has continued to shift to higher frequencies with time.

At the conclusion of this series of measurements the samples were tested for slipping by pulling them with a spring balance (in the line of the dynamic shearing forces) while they were still in position in the apparatus. At 1200 grams of force the samples began to slip. Since the maximum amplitude of the alternating shear force during measurements was 3.0 grams, it can be concluded that slipping did not contribute to the results.

The samples were removed and annealed in an air oven for 15 hours at 140–150°C and reinserted in the apparatus after three days at room temperature

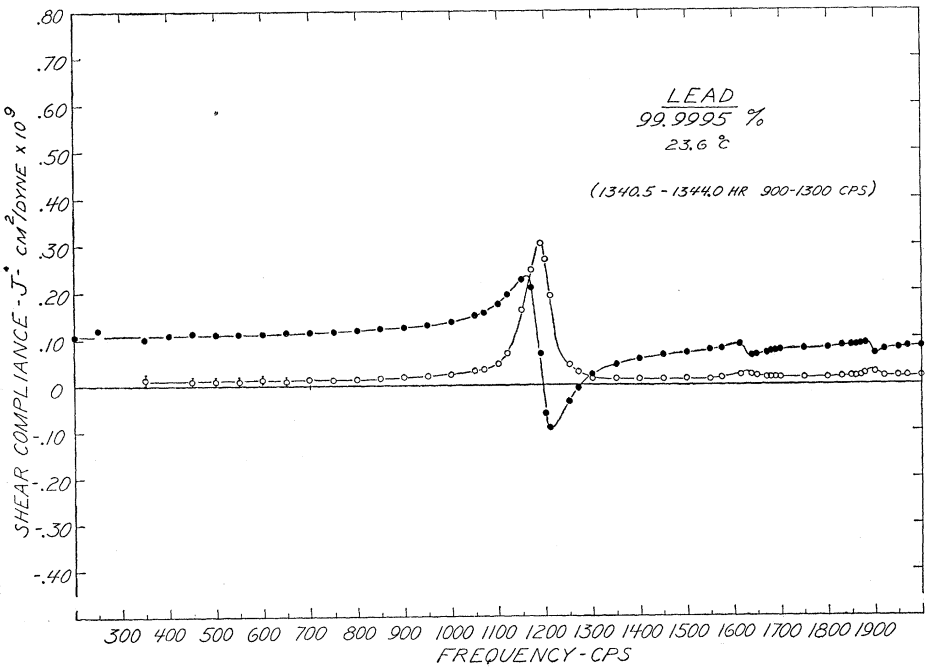

FIG. 13. Variation of the complex shear compliance ($\mathbf{J}^* = J' - iJ''$) with frequency for the polycrystalline lead of Fig. 8 at the time (~1350 hr) and temperature indicated. Solid circles, J'; open circles, J''.

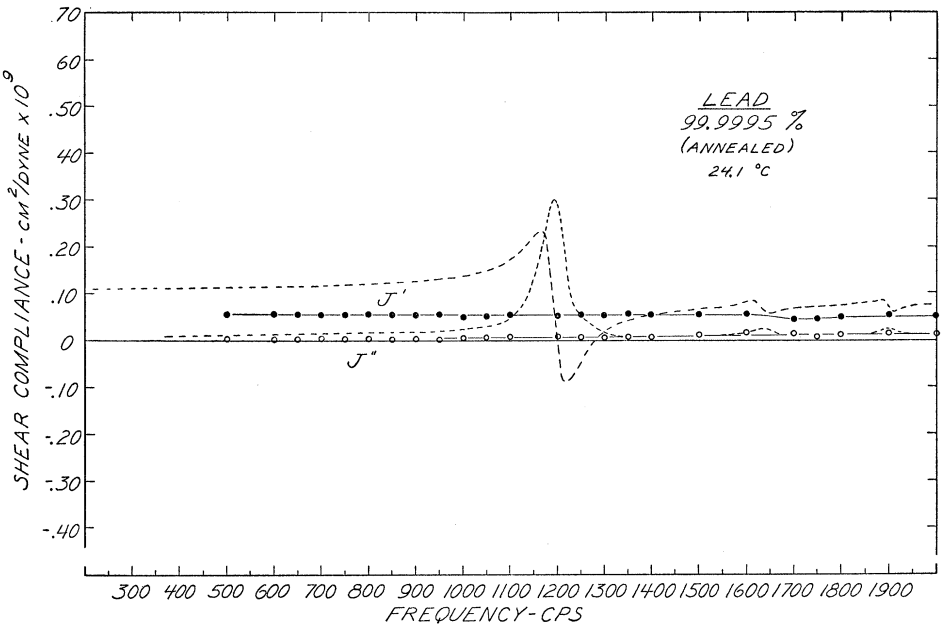

FIG. 14. Variation of the complex shear compliance ($J^*=J'-iJ''$) with frequency for the polycrystalline lead of Fig. 8 after annealing. Solid circles, J'; open circles, J''. The data of Fig. 13 taken before annealing is indicated by the dashed lines.

(~24°C). The results on the annealed samples (No. 22a) are shown in Figs. 14 and 15. The only resonance now observed is that at 2900 cps. The general level of the compliance at other frequencies has decreased. The samples were again tested for slipping which began at 1300 grams of force. This is an indirect indication that the static compressive force on the samples was the same as that during the previous measurements, as well as demonstrating that the samples were not slipping during the dynamic measurements (in which the maximum amplitude of the shearing force was again 3.0 grams).

Samples of lead machined from the same cast bar but of different dimensions (No. 25, see Table I) were measured from 500 to 4000 cps, showing a very small resonance at 2825 cps and a large resonance (of the same order of magnitude as that previously found at 2900 cps) in the neighborhood of 3500 cps. The general

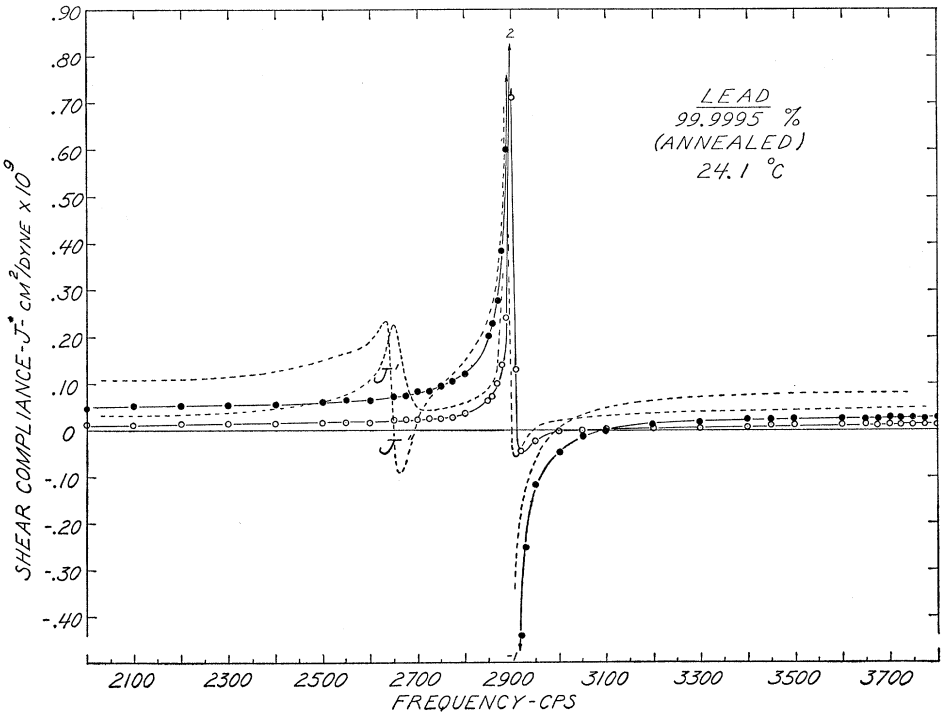

FIG. 15. Variation of the complex shear compliance ($J^*=J'-iJ''$) with frequency for the polycrystalline lead of Fig. 8 after annealing. Solid circles, J'; open circles, J''. The data of Fig. 12 taken before annealing is indicated by the dashed lines.

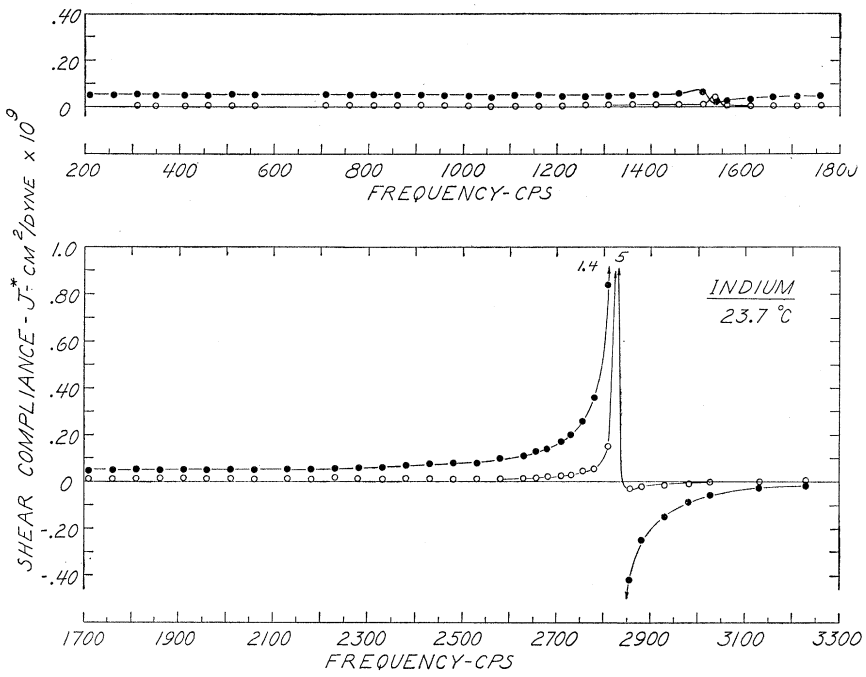

FIG. 16. Variation of the complex shear compliance ($J^*=J'-iJ''$) with frequency for polycrystalline indium. Solid circles, J'; open circles, J''. Analysis of indium; Zn, 0.01%; Sn, 0.01%; Cu, 0.006%; Pb, trace.

level of compliance was the same as that for the previous annealed samples (No. 22a). When annealed for 24 hours at 150°C in an air oven and remeasured, these samples still exhibited a large resonance near 3550 cps but no other appreciable dispersion in the 500 to 4000 cps region. The general level of the compliance remained the same.

A third set of lead samples machined from the opposite end of the cast bar, and of dimensions identical to the first set, exhibited a large, very sharp resonance at 2815 cps and a small resonance at 3650 cps but no other dispersion in the range 200 to 4200 cps.

2. Indium

Samples of polycrystalline indium of 99.984% purity (No. 23, see Table I) were compressed 4% in transducer I; measurements at 23.7°C began at 100 cps 5.2 hours later and continued to 1350 cps at 9.0 hours after compression. From 23.0 to 31.5 hours, measurements were made in the frequency range of 1350 to 3200 cps. The results are shown in Fig. 16. From Fig. 16 it is evident that only one very small dispersion region exists in the region 200 to 2000 cps, i.e., at 1540 cps. Experimental points are missing at 600 to 650 cps because the total

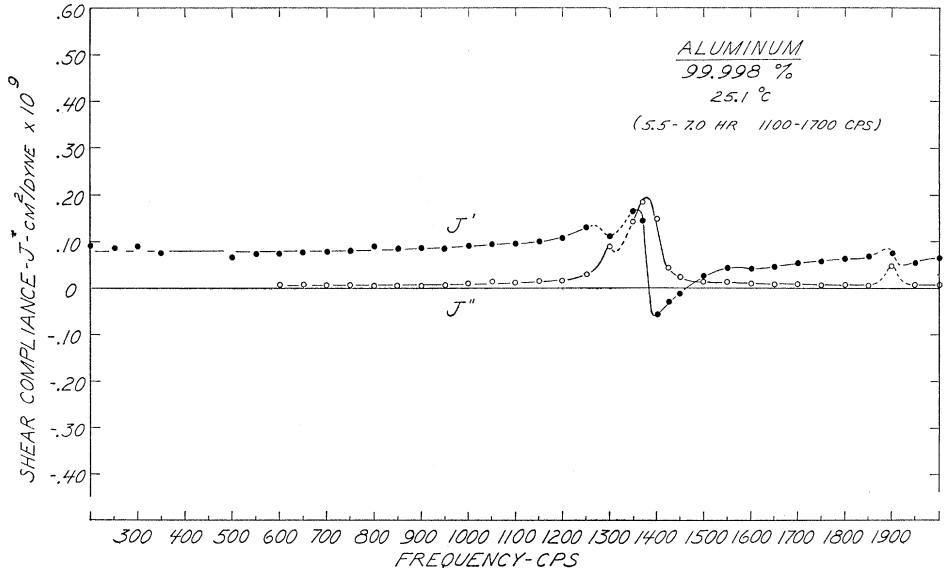

FIG. 17. Variation of the complex shear compliance ($J^*=J'-iJ''$) with frequency for polycrystalline aluminum. Solid circles, J'; open circles, J''. Probable impurities in aluminum: Fe, Si, Cu; total impurities known to be less than 0.002%.

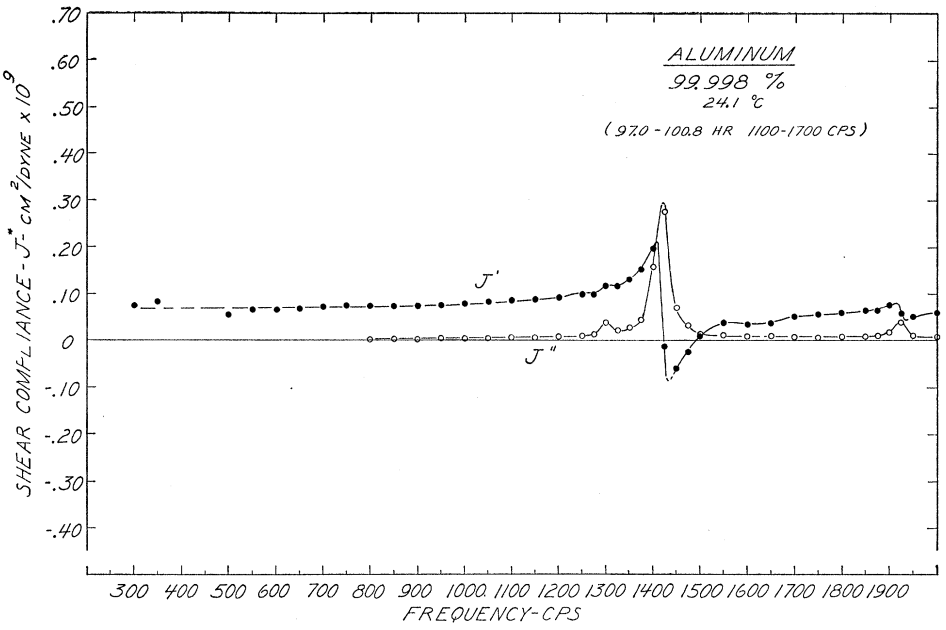

FIG. 18. Variation of the complex shear compliance ($J^* = J' - iJ''$) with frequency for the polycrystalline aluminum of Fig. 17. Solid circles, J'; open circles, J''.

mechanical admittance of the system ($\mathbf{Y}_M$) was almost zero in this region, making an accurate determination of the complex shear compliance of the sample impossible. It is certain that the values of J' and J'' are small in this region however. Values of J' from 100 to 200 cps (not shown in Fig. 16) remained at approximately 0.05×10^{-9} cm²/dyne. Values of J'' below 1200 cps were too small to be determined exactly but are known to be less than 0.005×10^{-9} cm²/dyne.

A large, very sharp, resonance is observed at 2830 cps which is similar to that found for lead at 2890 cps.

At the conclusion of measurements, the samples were tested for slipping by inserting a double hook to engage the samples and pulling with a spring balance (in the direction of the dynamic shearing forces) while the samples were in position in the apparatus. A force of 2000 grams was not sufficient to pull the samples loose while the maximum amplitude of the alternating shear

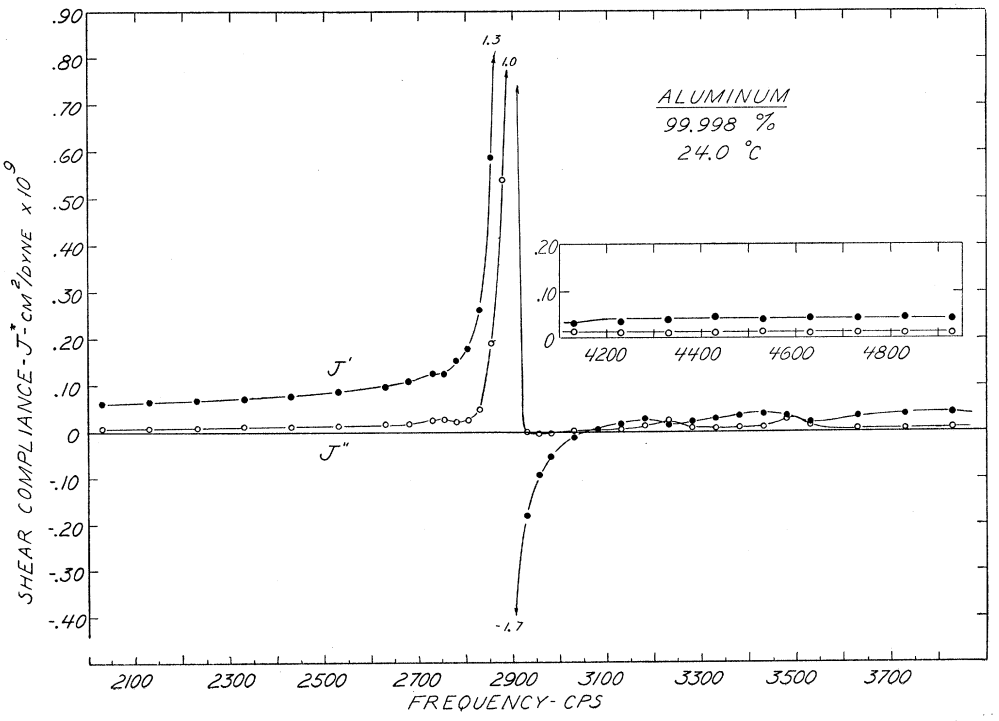

FIG. 19. Variation of the complex shear compliance ($J^* = J' - iJ''$) with frequency for the polycrystalline aluminum of Fig. 17. Solid circles, J'; open circles, J''.

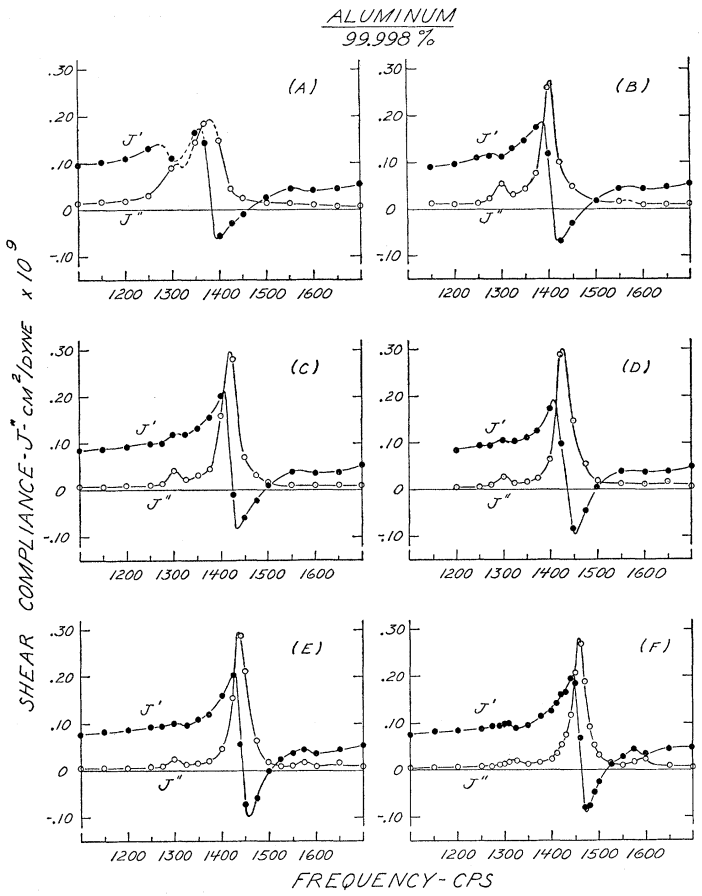

FIG. 20. Variation of the complex shear compliance ($\mathbf{J}^*=J'-iJ''$) with frequency for the aluminum of Fig. 17 at different times after initial static compression (1.9%) in the apparatus. (*A*) 5.5 to 7.5 hr, (*B*) 25.8 to 26.5 hr, (*C*) 97.90 to 100.8 hr, (*D*) 267.8 to 270.0 hr, (*E*) 475.5 to 462.0 hr, (*F*) 647.0 to 652.2 hr. Solid circles, J'; open circles, J''.

during force measurements was 3.0 grams; hence slipping was not a factor in the results. In fact, the samples had to be knocked loose from the floating-mass sample holders to which they had become firmly attached.

After removal the samples were found to have a permanent deformation of 2% in the direction of static compression.

3. Aluminum

Samples of polycrystalline aluminum of 99.998% purity (No. 24 of Table I) were compressed 1.9% in transducer I and the first set of measurements taken from 100 to 2000 cps 0.20 to 7.8 hours after compression. The results are shown in Fig. 17. A double resonance at 1315 and 1395 cps and a small resonance at 1915 cps are evident. The results of subsequent measurements from 300 to 2000 cps at 94.5 to 102.5 hours, from 2000 to 3600 at 106.5 to 109.5 hours, and from 3600 to 5000 cps at 240.5 to 247.0 hours are shown in Figs. 18 and 19. In addition to resonances at 1315, 1435, and 1940 cps a large resonance is observed at 2890 cps as was the case for lead (No. 22, 22a).

The doublet in the vicinity of 1400 cps is of particular interest because of the manner in which the high-frequency resonance increases as the low-frequency peak decreases. The region from 100 to 1700 cps is shown during six different time intervals in Fig. 20.

Measurements from 2000 to 4000 cps taken about 500 hours after compression were almost identical to those shown in Fig. 19.

The aluminum samples were tested for slipping at the conclusion of the measurements with the result that no slipping occurred with a force of 2000 grams. After removal from the apparatus the samples were found to have no permanent deformation.

4. Experimental Error

The values of electrical impedance from which the mechanical admittance is calculated [Eq. (7)] are determined to within $\frac{1}{2}$ to 1% using the calibrated bridge circuit of Fig. 4. At each frequency four independent bridge balances are made by varying R_3 and R_A from which two independent values of $\mathbf{Z}_{12}$ are obtained. These generally agree to within 1% or less. This does not mean that the sample admittance can be determined with the same precision, however, Two subtractions are involved in arriving at the value of the sample admittance as previously described in Sec. II, 1. When either of these differences is small the results are correspondingly uncertain even though each of the

quantities involved in the subtraction is itself precisely known. In the present case at low frequencies (<100 cps) the driving tube and suspended mass oscillate essentially as a single rigid unit whose motion is independent of sample properties. As the frequency increases, however, the admittance of the suspended mass decreases so that the difference $(\mathbf{Y}_{AB}-\mathbf{Y}_{Mm})$ becomes large. Over most of the range $\mathbf{Y}_{Mm}$ is less than 10% of $\mathbf{Y}_{AB}$ and the values of compliance are estimated to be accurate to within ±3%. At the highest frequencies the impedance of the driving tube itself predominates and the results again become increasingly uncertain. The estimated uncertainty in the data is ±3% unless otherwise indicated.

The frequency of each measurement was set by comparison with standard frequencies of 10, 100, 1000, or 10 000 cps obtained from a Hewlett Packard Model 100D Low-Frequency Standard or, in later measurements, by means of a Hewlett Packard Model 523B Electronic Counter. The estimated uncertainty in any frequency reported is less than ±2 cps.

IV. DISCUSSION

1. Apparatus as a Possible Source of the Resonances

Because of the unusual and unpredicted resonances observed, it is natural to suspect that the results are somehow due to the apparatus or method of measurement rather than to any intrinsic properties of the materials. In this connection the following comments are relevant:

(1) The behavior of the transducer system without samples is regular and agrees closely with that predicted from the mechanical model alleged to represent the system (Fig. 3). In particular, when the shearing faces of the apparatus are clamped directly together, and the mechanical admittance of the clamped system measured at closely spaced frequencies, no resonances in the mechanical admittance are observed and the deviation from ideal clamped behavior is very small (Figs. 5–6).

(2) Measurements on many amorphous polymers made on this and similar apparatuses[13–16] have not resulted in the discovery of resonances of this type. The previous measurements have been made at fairly small frequency intervals although not as small as in the present work. While the materials previously measured have been essentially noncrystalline, they have included hard, glassy materials in the same general compliance range (10^{-10} cm²/dyne) as the pure metals of this study. Measurements at 25°C from 100 to 2000 cps on polyisobutylene in this apparatus at very closely spaced frequencies have shown no resonances in the compliance.

(3) The position and magnitude of some of the resonances observed in lead and aluminum change with time. It is difficult to see how this time dependence can be attributed to the apparatus.

(4) Four of the five resonances observed in lead were removed by annealing the samples for 15 hours at 140°C. Since the samples were annealed while removed from the apparatus, it is most probable that these resonances, at least, resulted from some preannealed condition of the sample material rather than from the apparatus.

(5) Samples of lead of different dimensions did not exhibit resonances at the same frequencies. This leads

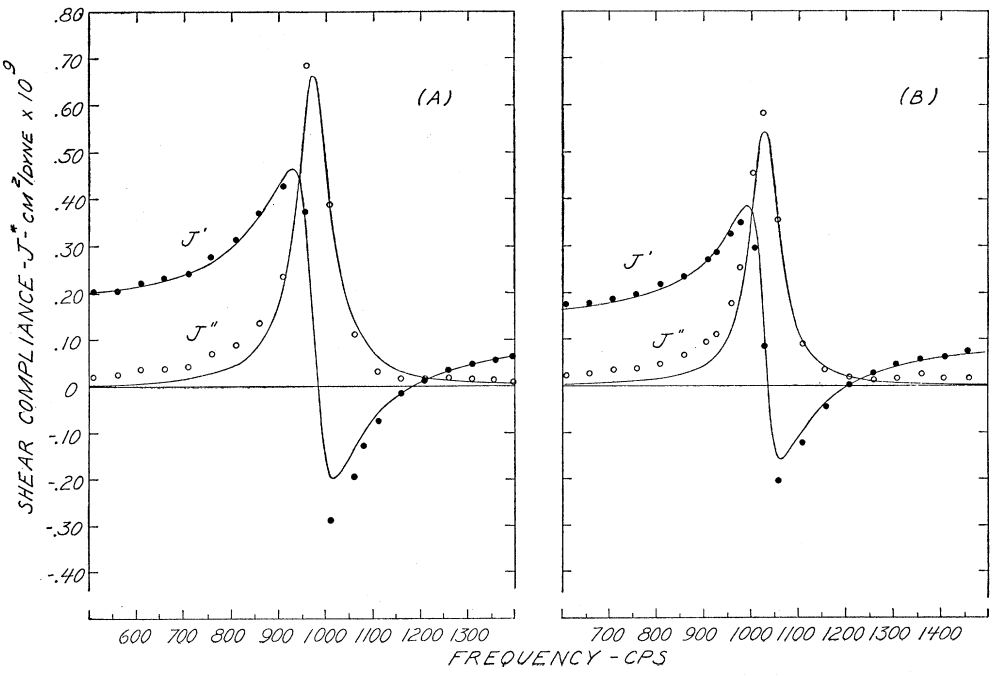

FIG. 21. Comparison of calculated values of compliance based on the model of Fig. 2 (solid lines) and experimental results for the first (low frequency) resonance in lead. Solid points, measured values of J'; open points, measured values of J''. (*A*) results at 22 hr, (*B*) results at 118 hr. The calculated curves are based on the empirical constants listed in Table II.

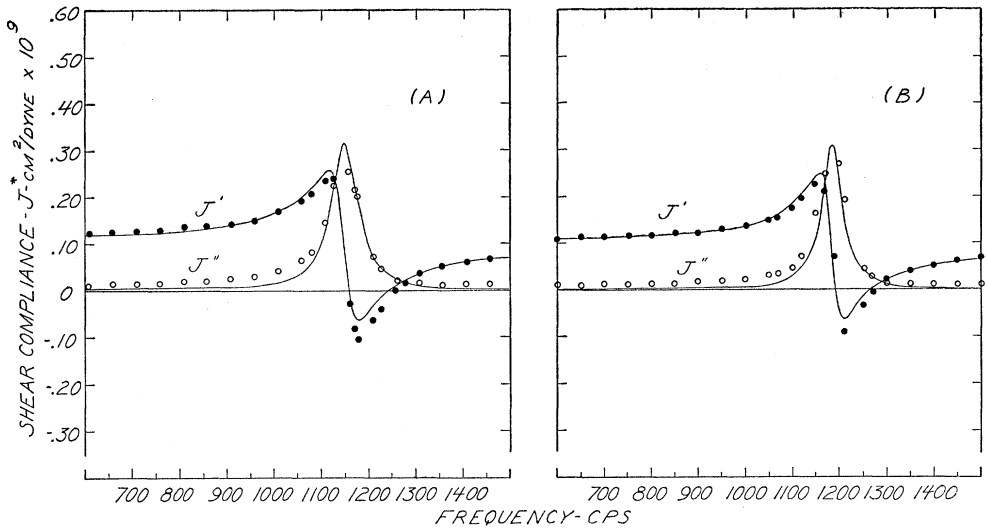

FIG. 22. Comparison of calculated values of compliance based on the model of Fig. 2 (solid lines) and experimental results for the first resonance in lead. Solid points, measured values of J'; open points, measured values of J''. (*A*) results at 644 hr, (*B*) results at 1350 hr. The calculated curves are based on the empirical constants listed in Table II.

to speculation that the resonances may be due to coupling between the shear vibration and other modes of oscillation of the sample. Additional tests on the effect of sample size are needed, however, before any definite conclusions can be drawn since it is not certain that the samples of lead were, in fact, structurally identical (e.g., they could have different dislocation densities) though machined from the same cast bar. In fact, samples of nearly identical dimensions machined from opposite ends of the cast bar did not give identical results.

In consequence of the above facts and a number of other tests on the apparatus, it has been concluded that the apparatus, as such, is not responsible for the observed phenomena.

2. Analysis of Dispersion Data for Lead

The observed dispersions have been noted to be very similar to the type of resonance dispersion to be expected from the mechanical model of Fig. 2. Accordingly, values of the constants of Fig. 2 and Eq. (2) were chosen to give the best fit to the experimental data for the first (lowest frequency) peak observed in lead. The values of J' and J'' calculated according to Eq. 2 are compared with the observed values in Figs. 21 and 22 and the values of the constants empirically selected are presented in Table II. The fit to the experimental data using the simple resonance equations is seen to be good although not exact. Values of J' just below and just above the resonant frequency are higher than the observed values and the observed values of J'' just below the resonant frequency are higher than those predicted. From Table II it can be seen that the values of τ, G, G_0, and η are of the order of magnitude to be expected but that the values of m/l are extremely large. The retardation time τ decreases with time while values of G, G_0, and m/l increase.

Although detailed analyses were not made of the resonances at 1630, 1880, and 2640 cps (Figs. 9 and 10), they appear to be of the same general type as the first (lowest frequency) resonance. These resonances also change in position and magnitude with time.

The resonance first observed at 2890 cps (Fig. 10) did not shift with time (Fig. 12) and was not noticeably affected by the annealing treatment (Fig. 15). The asymmetry of the J'' *vs* frequency peak is pronounced in this resonance and values of J'' become slightly negative in passing through a shallow minimum at frequencies just above the large maximum (Figs. 10, 12, and 15). A similar resonance was obtained with aluminum samples of the same dimensions ($\frac{1}{4}$ in. diam $\times\frac{1}{5}$ in. thick) as shown in Fig. 18. The resonance at 2830 cps in indium samples of different dimensions ($\frac{3}{8}$ in. diam$\times\frac{1}{5}$ in. thick) is of the same type. Negative values of J'' found in these three instances indicate that

TABLE II. Analysis of dispersion data for lead[a] based on the mechanical model of Fig. 2 [Eq. (2)].

Time after compression (hr)	22	118	644	1350
Resonant frequency, f_r (cps)	975	1030	1150	1185
Retardation time, τ (sec)	1.45×10^{-5}	1.15×10^{-5}	0.80×10^{-5}	0.60×10^{-5}
Retarded modulus, G (dynes/cm²)	1.7×10^{10}	2.5×10^{10}	5.5×10^{10}	7.1×10^{10}
$1/G$ (cm²/dyne)	0.060×10^{-9}	0.040×10^{-9}	0.018×10^{-9}	0.014×10^{-9}
Instantaneous modulus, G_0 (dynes/cm²)	8.3×10^{9}	9.5×10^{9}	10×10^{9}	11×10^{9}
$1/G_0$ (cm²/dyne)	1.20×10^{-9}	0.105×10^{-9}	0.095×10^{-9}	0.090×10^{-9}
Effective mass per unit length, m/l (grams/cm)	453	597	1050	1280
Viscosity, η (dyne-sec/cm)	2.5×10^{5}	2.9×10^{5}	4.4×10^{5}	4.3×10^{5}

[a] $1/\omega\eta_0$ is assumed to be negligible in this analysis.

energy is being given up by the vibrating system. The resonance observed near 3500 cps in the second set of lead samples ($\frac{3}{8}$ in. diam$\times$0.15 in. thick) is of this type also. These particular resonances are tentatively ascribed to coupling between the shear vibration and another mode or modes of oscillation of the samples. They appear to depend on the sample shape and material[22] but to be independent of time and annealing treatment.

3. Dislocations as a Possible Source of the Resonances

The changes with time and the effect of annealing (observed for the lead samples) suggest that the resonances observed below 2800 cps in lead and aluminum may result from dislocation vibrations. Mott and Nabarro[23] calculate the frequency with which a straight dislocation in a hard metal vibrates about its mean position to be of the order of 10^8 to 10^9 cps. They consider a precipitation-hardened metal with line dislocations arrested at the sites of precipitate atoms which are about 200 Angstrom apart. Smith[24] points out that this value of frequency will decrease with increasing distance between the points at which the dislocation is temporarily arrested, but estimates that even with metals of very high purity this frequency would not be less than 10^4 to 10^5 cps. However, Lomnitz[25,26] reports that creep tests in igneous rocks indicate a value close to 1000 cps for this vibration frequency. Various theories[20, 27–29] of the effect of dislocations on dynamic mechanical properties have been advanced but these fail to predict any resonances or appreciable dispersion of any sort of audio-frequencies.

The time variation of the resonances observed in lead (i.e., those below 2800 cps) is consistent with the idea that dislocations are responsible for the dispersion. Dislocations originally present in the cast lead or introduced as a result of machining, or of the static stress applied in the apparatus would gradually anneal out with time even at room temperature since recrystallization is known to take place in lead anywhere above 0°C. Thus, the gradual decrease in the amplitude of the first (lowest frequency) resonance may result from a decrease in the number of dislocations or from a change in dislocation vibration frequency as a result of a decrease in the size of a particular type of dislocation.

From Figs. 8, 9, 11, and 13 it is apparent that not only does the magnitude of the resonance decrease, but the general levels of J'' and J' at frequencies below the first resonance decrease with time as well. This may be related to what Nowick[27] has called the "Koster effect" in which a decrease in internal friction ($\sim J''/J'$) of cold-worked metals is observed as a result of low-temperature annealing. From the data shown, however, it is obvious that observations at a single or widely spaced frequencies such as those previously reported are inadequate for the description of the effect of cold working on dynamic mechanical properties such as the loss compliance (or internal friction).

The time variation of the observed resonance in the region of 1400 cps in aluminum (Fig. 19) is not as great as that for lead. This again is reasonable since the recrystallization rate for aluminum is negligible at temperatures below 150°C. An interesting feature of the aluminum data is the manner in which the peak in J'' originally found near 1400 cps increases as the maximum at 1300 cps decreases. A third peak at 1590 cps is evident in data taken at later times but may have actually been present at the outset. (Experimental points in this region were not as closely spaced in the earlier measurements.) A more detailed treatment of the aluminum data will be presented in a subsequent paper.

While it is easy enough to explain the *variation* of the observed phenomena with time, high-temperature annealing, and cold work in terms of some dislocation mechanism, the occurrence of the resonances themselves is difficult to explain. If we consider the theory of Granato and Lücke,[20] for example, as applying to a polycrystalline metal in which there exists a network of dislocations, a resonant frequency, f_0, is predicted such that $f_0=(1/2L)(C/A)^{\frac{1}{2}}$, where C is the effective tension in a dislocation loop of length L, and A is the effective mass per unit length. For a loop length of 10^{-4} cm this theory (which is equivalent to considering the dislocation lines as vibrating strings) predicts a resonance in lead at 2.0×10^8 cps.

The analyses of the experimental data for lead based on the model of Fig. 2 demonstrate that the low-frequency resonances are due to large values of m/l rather than small values of shear modulus and hence C. In order to obtain resonant frequencies of 10^3 cps on the basis of the Granato-Lücke theory, values of L of the order of 20 cm would be needed, or much larger values of A would have to be postulated; i.e., A would have to be increased from 3.16×10^{-15} to 1.44×10^{-4} gram/cm. Since $A=\pi\rho a^2$, where ρ is the density and a is the Burgers vector, this could be accomplished only by increasing a. This however would result in a corresponding increase in $C=2Ga^2/\pi(1-\nu)$ (where G equals the shear modulus and ν is Poisson's ratio) and therefore no decrease in f_0.

---

[22] Measurements on polyethylene samples (72% crystallinity) ($\frac{1}{4}$ in. diam.$\times\frac{1}{8}$ in. thick) show this type of resonance at 2725 cps but values of J'' at the minimum remain positive.

[23] N. F. Mott and F. R. N. Nabarro, *Report of the Conference on Strength of Solids* (Physical Society, London, 1948), Vol. 1.

[24] C. L. Smith, Proc. Phys. Soc. (London) **61**, 201 (1948).

[25] C. Lomnitz, J. Geol. **64**, 473 (1956).

[26] C. Lomnitz, J. Appl. Phys. **28**, 201 (1957).

[27] A. S. Nowick, J. Appl. Phys. **25**, 1129 (1954).

[28] J. Weertman, J. Appl. Phys. **26**, 202 (1955).

[29] E. W. Montroll and R. B. Potts, Phys. Rev. **100**, 525 (1955).

4. Mechanical Resonance Dispersion in Crystalline Polymers

Measurements of the shear compliance of crystalline polymers[30] made on the apparatus have resulted in the discovery of similar resonance dispersions for polytetrafluorethylene (Teflon), polyvinyl stearate, and crystalline polyethylene. In the case of Teflon, nearly identical results have been obtained for samples of different dimensions which were subjected to similar cold-working and thermal treatments. The effect of pressure and temperature have also been studied. While a detailed treatment of these data will be given elsewhere, it is interesting to note, in connection with the results on metals, that a time dependence and effect of annealing are found for crystalline polymers as well as for metals.

V. CONCLUSIONS

Measurements of the complex shear compliance of pure polycrystalline metals have resulted in the discovery of multiple resonance dispersions in the audio-frequency range.

Since previous experimental work has not included the measurement of the shear compliance of pure polycrystalline metals at closely spaced frequencies in this range, the results are not in contradiction with any previous experimental evidence.

Results on lead indicate that all but one of the resonances may be eliminated by high-temperature annealing; some of the resonances are time dependent indicating that annealing is taking place at room temperature.

Analysis of the data on the basis of a simple mechanical model, consisting of an instantaneous or ideal spring in series with a retarded (viscoelastic) spring, gives a remarkably close fit. On this basis, the low-frequency dispersions seem to result from unusually large values of effective mass per unit length rather than from small values of shear modulus.

The possibility that dislocation vibrations are responsible for the observed phenomena is considered but no specific mechanism is found to explain the results. A number of the present theories concerning dislocation vibrations are examined but these uniformly fail to predict any mechanical dispersion at audio-frequencies. It is suggested that present dislocation theories be re-examined in view of the experimental results presented here.

In addition to their theoretical implications the results are of the utmost practical significance since they indicate that certain materials subject to mechanical vibrations of relatively low frequencies may undergo tremendous changes in modulus at a particular frequency or frequencies.

VI. ACKNOWLEDGMENTS

This work was supported in part by a grant-in-aid from the B. F. Goodrich Company, Brecksville, Ohio. Mrs. Charles L. Reiser and Mrs. Donald C. Griesel assisted in calculations and in some of the measurements.

Discussions with J. A. Sauer and N. Fuschillo were particularly helpful during the course of the work and in attempts to explain the results. I am grateful to R. W. Lindsay, H. J. Read, and H. M. Davis for their help in obtaining pure samples of the metals studied.

[30] Edwin R. Fitzgerald, Bull. Am. Phys. Soc. Ser. II, **2**, 126 (1957); J. Chem. Phys. **27**, 1180 (1957).